EUROPEAN JOURNAL OF PURE AND APPLIED MATHEMATICS
2025, Vol. 18, Issue 4, Article Number 7067
ISSN 1307-5543 – ejpam.com
Published by New York Business Global

Threshold-Based Nonlinear Protocols for Scaled Edge Consensus under Input Saturation Constraints

Mana Donganont[1], Uamporn Witthayarat[1], Siriwan Intawichai[1], Saranya Phongchan[1,*]

[1] *Department of Mathematics, School of Science, University of Phayao, Phayao,56000, Thailand*

Abstract. Scaled edge consensus in strongly connected directed multi-agent systems subject to input saturation is examined. Departing from node-based formulations, edge-level dynamics are modeled on the line digraph with heterogeneous scaling, and a fully distributed threshold-based protocol is introduced wherein each edge updates its state using only local disagreements with neighboring edges. Three performance regimes are established: (i) in the unsaturated case, global scaled consensus is achieved; (ii) under saturation, consensus is preserved whenever a verifiable safe-dispersion bound on the initial condition holds; and (iii) for large initial disagreements, a low-gain design guarantees bounded quasi-consensus with an explicit radius. The analysis employs Lyapunov methods, Metzler and edge-Laplacian structure, and invariance principles. Simulations on a 10-node, 18-edge directed network corroborate the theory and reveal trade-offs among convergence speed, robustness to saturation, and consensus accuracy. The resulting framework underscores the utility of edge-level coordination under actuation limits and exhibits scalability for networked control, distributed coordination, and edge-centric information processing.

2020 Mathematics Subject Classifications: 93D50, 93D20, 93D40, 37N35
Key Words and Phrases: Edge consensus, scaled dynamics, input saturation, threshold activation, quasi-consensus, multi-agent systems

1. Introduction

Consensus in multi-agent systems (MASs) has become a central theme in distributed control, networked computation, and cooperative robotics. Since the seminal work of Olfati-Saber on flocking and consensus over dynamic graphs [1], the field has evolved beyond node-based averaging to encompass time delays, nonlinearities, constraints, and hybrid-time implementations. Classical protocols align agent (node) states, which is effective for many tasks but can obscure the physics of interactions—flows, couplings, or

*Corresponding author.
DOI: https://doi.org/10.29020/nybg.ejpam.v18i4.7067

Email addresses: mana.do@up.ac.th (M. Donganont), uamporn.wi@up.ac.th (U. Witthayarat), siriwan.in@up.ac.th (S. Intawichai), saranya.ph@up.ac.th (S. Phongchan)

conservation relations—occurring along network edges. As applications expand to vehicular platooning, power networks, robotic swarms, and wireless sensing, modeling and controlling the interactions themselves has proven advantageous.

This recognition has spurred edge-centric formulations in which dynamical states are assigned to the edges of the communication graph. Early formalizations of nonnegative edge (quasi-)consensus [2] and positive edge coordination [3, 4] demonstrate that regulating edge variables yields finer control granularity, natural symmetry, and compatibility with physical constraints. Actuation limits have been examined in edge settings with input saturation [5], and fixed-time as well as optimization-oriented perspectives have highlighted the algorithmic benefits of edge-level updates for speed and flexibility [6, 7]. These advances collectively point to edge-based coordination as an expressive alternative to node-centric consensus.

Beyond exact agreement, quasi-consensus has emerged as a practically relevant relaxation: agents (or edges) converge to a bounded neighborhood or to structured ratios rather than a single value. Node-based studies—addressing heterogeneity, packet loss, sampling, switching, or impulses—have mapped out much of this landscape [8–15]. A complementary direction is scaled consensus [16], in which asymptotic ratios are prescribed by nonuniform weights to enable task balancing and energy-aware objectives. The edge counterpart, scaled edge consensus, is comparatively recent: Park et al. [17] proposed a hybrid (CT/DT) framework with normalized scaling, while subsequent works explored pulse-modulated and complex-weighted extensions in hybrid settings [18–20]. However, most existing results either assume ideal actuators or treat scaling, thresholding, and saturation in isolation.

In practice, actuator saturation is unavoidable and strongly shapes closed-loop behavior, while threshold activation (or hysteresis) is desirable to reduce chatter, communication, and energy consumption by engaging control only when disagreements exceed meaningful levels. Designing protocols that are simultaneously scaled, threshold-based, and saturation-aware—while remaining fully distributed at the edge level—therefore addresses an important gap. This paper fills that gap by developing and analyzing a threshold-based protocol for scaled edge (quasi-)consensus in strongly connected directed MASs with input saturation. Edge states evolve on the line digraph and are updated using only local disagreements with neighboring edges. Heterogeneous scaling is encoded diagonally, and normalized coordinates render the notion of scaled consensus well-posed under heterogeneous interactions.

The contributions are threefold and integrated within a single, rigorously analyzed framework. First, we establish that the proposed protocol achieves global scaled consensus in the unsaturated regime, preserves consensus under saturation provided a verifiable safe-dispersion bound on the initial condition, and guarantees bounded quasi-consensus via a low-gain design in high-dispersion scenarios. Second, we clarify tuning and interpretability: thresholds and gains have transparent effects, with larger thresholds reducing activation and control energy, and lower gains enlarging robustness to saturation at the cost of accuracy; these trade-offs are formalized and the quasi-consensus radius is quantitatively characterized. Third, we validate the approach on a strongly connected directed

network with 10 nodes and 18 edges, where simulations corroborate the theory and expose speed–robustness–accuracy trade-offs, while the distributed structure scales naturally and remains compatible with hybrid-time extensions [17–19]. The analysis throughout employs Lyapunov and invariance arguments matched to Metzler and edge-Laplacian structure [2–5, 21, 22].

This study complements the node-based quasi-consensus and constrained-control literature [8–14] by moving the design locus to edges, following the expressiveness and performance motivations in [6, 7]. Relative to positive/nonnegative edge consensus with constraints [2–5], we explicitly incorporate heterogeneous scaling and threshold activation and provide unified guarantees across the unsaturated, safe-dispersion, and low-gain regimes. Our results are also complementary to recent hybrid and pulse-modulated developments [17–19], which emphasize temporal heterogeneity; here we focus on continuous-time operation under actuation limits while preserving a path to hybrid-time generalizations.

The scope of this paper adopts strong connectivity and positive scaling as standing assumptions; weight balance and switching topologies can be handled under additional joint-connectivity and dwell-time conditions discussed later. Stochastic disturbances, explicit delay margins, and fractional-memory effects are outside our main scope, although the threshold-based design is compatible with event-triggered and hybrid-time mechanisms and is amenable to richer models in future work.

The remainder of the paper is organized as follows. Section 2 introduces notation, directed graphs and line digraphs, and scaled edge consensus objectives. Section 3 presents the distributed threshold-based protocol and the saturation model. Section 4 develops Lyapunov and invariance analyses for the three operating regimes. Section 5 reports simulations highlighting convergence speed, robustness to saturation, and accuracy trade-offs. Section 6 concludes and outlines extensions to switching graphs, event-triggered communication, and hybrid-time operation.

2. Preliminaries and Problem Formulation

Mathematical Notation and Basic Concepts

Let $\mathbb{R}$ denote the field of real numbers; $\mathbb{R}^N$ and $\mathbb{R}^{N\times N}$ denote, respectively, the spaces of real column vectors and real square matrices of dimension N. For $x \in \mathbb{R}^N$, $\|x\|_2$ denotes the Euclidean norm. The vectors $\mathbf{1}_N$ and $\mathbf{0}_N$ are the all-ones and all-zeros vectors of dimension N; I_N is the $N \times N$ identity. A matrix $A \in \mathbb{R}^{N\times N}$ is *nonnegative*, written $A \geq 0$, if all entries are nonnegative; it is *Metzler* if all off-diagonal entries are nonnegative. A matrix is *row-stochastic* if $A \geq 0$ and $A\mathbf{1}_N = \mathbf{1}_N$.

To improve readability, we collect recurrent symbols in a compact notation map:

Symbol	Meaning
$\mathcal{G} = (\mathcal{V}, \mathcal{E})$	Directed communication graph (digraph), $\lvert\mathcal{V}\rvert = N$, $\lvert\mathcal{E}\rvert = M$
$\mathcal{L}(\mathcal{G})$	Line digraph whose nodes index edges of $\mathcal{G}$
$A \in \mathbb{R}^{N\times N}$	Adjacency of $\mathcal{G}$, $(i,j) \in \mathcal{E} \iff a_{ij} = 1$
$B \in \mathbb{R}^{N\times M}$	Incidence matrix of $\mathcal{G}$ (tail/head convention fixed below)
$L_e \in \mathbb{R}^{M\times M}$	Edge Laplacian (operator on $\mathcal{L}(\mathcal{G})$)
$X \in \mathbb{R}^{M}$	Edge state vector with entries x_{e_k}, $e_k \in \mathcal{E}$
$D_s = \mathrm{diag}(s_{e_1}, \ldots, s_{e_M}) \succ 0$	Heterogeneous edge scaling
$Z = D_s^{-1} X$	Normalized edge coordinates
$\alpha \geq 0$	Disagreement threshold for activation
$\omega > 0$	Actuation saturation level
$\gamma > 0$ (and $\varepsilon \in (0,1]$)	Control gain (and low-gain factor)

Directed Graphs, Line Digraph, and Edge Operators

We consider a *strongly connected* digraph $\mathcal{G} = (\mathcal{V}, \mathcal{E})$ with nodes $\mathcal{V} = \{1, \ldots, N\}$ and directed edges $\mathcal{E} \subseteq \mathcal{V} \times \mathcal{V}$. A directed edge from j to i is denoted $(i,j) \in \mathcal{E}$. The in-neighborhood of i is $\mathcal{N}_{\mathrm{in}}(i) := \{\, j : (i,j) \in \mathcal{E} \,\}$. We adopt a fixed tail/head convention for the incidence matrix $B = [b_{ik}]$, where $b_{ik} = +1$ if node i is the head of edge e_k, $b_{ik} = -1$ if node i is the tail of e_k, and $b_{ik} = 0$ otherwise.

The *line digraph* $\mathcal{L}(\mathcal{G}) = (\mathcal{V}_e, \mathcal{E}_e)$ is defined by $\mathcal{V}_e = \mathcal{E}$; there is an arc from $e_k = (j,k)$ to $e_\ell = (i,j)$ if and only if the head of e_k coincides with the tail of e_ℓ (i.e., $k = i$). This construction captures edge-to-edge interactions and induces linear operators on $\mathbb{R}^M$. Throughout, L_e denotes an *edge Laplacian* consistent with $\mathcal{L}(\mathcal{G})$ and the choice of interaction weights; its off-diagonal entries are nonnegative (Metzler) and row sums are zero on the active interaction graph. The symmetric part of the active operator is positive semidefinite, and $\ker L_e = \mathrm{span}\{\mathbf{1}_M\}$ on each strongly connected active component. These properties will be used to construct Lyapunov functions and to apply invariance principles.

Assumption 1 (Standing connectivity)**.** *The base digraph $\mathcal{G}$ is strongly connected. For time-varying activation patterns (due to thresholding), the induced active line-digraph is* jointly strongly connected *with an average dwell-time bound. Under this joint-connectivity, the invariant subspace associated with L_e remains* $\mathrm{span}\{\mathbf{1}_M\}$ *in the aggregate sense.*

Remark (Weight balance and switching). If $\mathcal{G}$ is weight-balanced, standard symmetrization yields sharper spectral estimates; for switching among a finite set of strongly connected graphs, Assumption 1 holds under classical joint-connectivity/dwell-time conditions.

Edge States, Scaling, and Consensus Formulation

In an edge-centric modeling framework, each directed edge $e = (i,j) \in \mathcal{E}$ is assigned a scalar state $x_{ij}(t) \in \mathbb{R}$ that evolves with time. Let the total number of directed edges be $M = \lvert\mathcal{E}\rvert$. Stacking the edge states in a fixed order yields the aggregate edge-state vector

$$X(t) = \big[x_{e_1}(t), \ldots, x_{e_M}(t)\big]^\top \in \mathbb{R}^M, \qquad \dot{X}(t) = U(t), \tag{1}$$

where $U(t) \in \mathbb{R}^M$ denotes the control input vector, which is constructed using only edge-local information available on the line digraph $\mathcal{L}(\mathcal{G})$.

Heterogeneity in edge interactions is captured through a positive definite diagonal matrix $D_s \succ 0$, referred to as the *scaling matrix*. The corresponding normalized edge coordinates are defined by

$$Z(t) := D_s^{-1} X(t). \tag{2}$$

The network is said to achieve **scaled edge consensus** if there exists a scalar $\lambda \in \mathbb{R}$ satisfying

$$\lim_{t\to\infty} Z(t) = \lambda \mathbf{1}_M \quad \Longleftrightarrow \quad \lim_{t\to\infty} \left(\frac{x_{ij}(t)}{s_{ij}} - \frac{x_{kl}(t)}{s_{kl}} \right) = 0, \quad \forall (i,j),(k,l) \in \mathcal{E}, \tag{3}$$

where s_{ij} represents the scaling coefficient associated with edge (i, j). The scalar λ corresponds to a *weighted steady-state value* determined by the left eigenvector of the scaled edge operator, and it depends explicitly on both the network topology and the scaling matrix D_s.

In the presence of input constraints or substantial initial dispersion, exact consensus may not be attainable. In such situations, the relaxed concept of **scaled edge quasi-consensus** is considered. Scaled edge quasi-consensus with radius $\rho > 0$ is said to hold if, for all sufficiently large t,

$$\max_{k,\ell} \left| Z_k(t) - Z_\ell(t) \right| \leq \rho, \tag{4}$$

and the set

$$\Omega_\rho := \{ Z \in \mathbb{R}^M : \max_{k,\ell} |Z_k - Z_\ell| \leq \rho \}$$

is forward invariant under the closed-loop dynamics. Under this condition, the normalized edge states converge to a bounded neighborhood of consensus rather than achieving exact alignment.

Saturation, Threshold Activation, and Solution Concept

In practical settings, physical actuators are subject to hard constraints, limiting the magnitude of admissible control inputs. This phenomenon is modeled via a symmetric saturation function defined by

$$\mathrm{sat}_\omega(v) := \mathrm{sign}(v) \cdot \min\{|v|, \omega\}, \qquad \omega > 0, \tag{5}$$

where ω denotes the saturation threshold.

To mitigate excessive control updates and reduce communication overhead, edge-to-edge interactions are governed by a *threshold-based activation mechanism*. Specifically, a coupling is activated only when the corresponding local disagreement exceeds a prescribed threshold $\alpha \geq 0$. The activation pattern is encoded in a diagonal (or suitably structured) matrix $\Phi_\alpha(Z) \in \mathbb{R}^{M\times M}$, whose e^{th} diagonal entry is equal to one if the local mismatch on edge e in the line digraph $\mathcal{L}(\mathcal{G})$ exceeds α, and zero otherwise.

Under this framework, the distributed edge protocol is defined by the following nonlinear control law:

$$\dot{X}(t) = \mathrm{sat}_\omega\left(-\gamma\,\Phi_\alpha(Z(t))\,L_e\,Z(t)\right), \qquad Z(t) = D_s^{-1}X(t), \qquad \gamma > 0, \tag{6}$$

where $L_e \in \mathbb{R}^{M\times M}$ denotes the edge Laplacian, and $D_s \succ 0$ is the scaling matrix introduced previously.

In scenarios characterized by large initial dispersion or tight input constraints, robustness can be enhanced through a low-gain modification of the control protocol:

$$\dot{X}(t) = \mathrm{sat}_\omega\left(-\varepsilon\,\gamma\,\Phi_\alpha(Z(t))\,L_e\,Z(t)\right), \qquad 0 < \varepsilon \le 1, \tag{7}$$

where ε serves as a gain-scaling parameter that moderates control intensity at the expense of convergence speed and precision.

Due to the discontinuities introduced by threshold activation and saturation, solutions to the above systems are interpreted in the *Carathéodory sense*, which accommodates discontinuous vector fields with well-defined limits almost everywhere. In cases involving set-valued right-hand sides—such as those arising from hysteresis or saturation kinks—solutions are further interpreted via *Filippov regularization*. These interpretations ensure the existence, continuity, and closure of system trajectories across activation and deactivation events and provide a rigorous foundation for the application of invariance principles in discontinuous dynamical systems.

Dispersion Measures and Safe-Dispersion Bounds

The dispersion of the initial normalized edge state is measured by

$$\mathrm{disp}_0 := \max_{k,\ell} \left|Z_k(0) - Z_\ell(0)\right|. \tag{8}$$

A sufficient condition ensuring that the control input remains strictly within the saturation limit—thereby preserving the unsaturated dynamics governed by (6)—is given by

$$\mathrm{disp}_0 < \frac{\omega}{M-1}. \tag{9}$$

This condition guarantees that the magnitude of all control inputs is initially below the actuator bound ω, and since the protocol is designed to be non-expansive under unsaturated flow, saturation will remain inactive throughout the evolution.

Although condition (9) is conservative, it remains easily verifiable. To mitigate its conservativeness, Section 4 introduces *spectral tightenings* by replacing the coarse factor $(M-1)$ with graph- and operator-dependent quantities such as $\|L_e\|/\lambda_2(L_e)$, or degree-based bounds associated with the line digraph $\mathcal{L}(\mathcal{G})$. These refinements yield less restrictive safe-dispersion domains and lead to sharper bounds on the quasi-consensus radius in the presence of saturation.

Stability Tools

Two standard results concerning the stability of linear and discontinuous systems are recalled for subsequent analysis.

Lemma 1 (Metzler Stability [21])**.** *Let $A \in \mathbb{R}^{n\times n}$ be a Metzler matrix. Then the system $\dot{x} = Ax$ is globally asymptotically stable if and only if all eigenvalues of A have strictly negative real parts.*

Lemma 2 (LaSalle-Type Invariance Principle [22])**.** *Consider the nonlinear system $\dot{x} = f(x)$ with a continuously differentiable Lyapunov function $V : \mathbb{R}^n \to \mathbb{R}$ satisfying $\dot{V}(x) \leq 0$. Then, every trajectory converges to the largest weakly invariant set contained in $\{x \in \mathbb{R}^n : \dot{V}(x) = 0\}$. For systems with discontinuous right-hand sides interpreted in the Filippov sense, a similar invariance principle applies under standard regularity conditions.*

Problem Statement

Given a strongly connected digraph $\mathcal{G} = (\mathcal{V}, \mathcal{E})$, a positive definite scaling matrix $D_s \succ 0$, a threshold parameter $\alpha \geq 0$, and a saturation limit $\omega > 0$, the objective is to design a fully distributed edge-local control protocol of the form (6)–(7) operating on the line digraph $\mathcal{L}(\mathcal{G})$, satisfying the following control objectives:

(i) *Unsaturated regime:* Achieve global scaled edge consensus under the assumption that saturation remains inactive along the entire trajectory.

(ii) *Saturated but safe-dispersion regime:* Guarantee scaled consensus provided that the initial dispersion satisfies a verifiable safe-dispersion bound, ensuring saturation is never activated.

(iii) *High-dispersion regime:* Ensure bounded scaled edge quasi-consensus with an explicitly computable convergence radius under a low-gain controller configuration.

The theoretical analysis aims to derive sufficient conditions in terms of graph structure and gain parameters, characterize the dependence of the limiting consensus value λ on the topology and scaling matrix D_s, and precisely quantify the trade-offs among convergence rate, activation frequency, control energy expenditure, and robustness to actuator saturation. These contributions are developed rigorously in Sections 3–4 and validated through numerical simulations in Section 2.

3. Protocol Design

This section presents a fully distributed protocol that achieves scaled edge (quasi-)consensus on the line digraph $\mathcal{L}(\mathcal{G})$ under actuator saturation and threshold activation. We adhere to the notation in Section 2: the stacked edge state is $X \in \mathbb{R}^M$, heterogeneous scaling is $D_s \succ 0$, and the normalized coordinate is $Z = D_s^{-1}X$. Edge-to-edge couplings are mediated by the edge-Laplacian L_e and an activation operator $\Phi_\alpha(Z)$ defined from local disagreements. Throughout, Assumption 1 (standing connectivity) is in force.

Normalized Edge Dynamics and Local Disagreements

For each edge $e = (i, j) \in \mathcal{E}$, the scalar state $x_{ij}(t)$ evolves as an integrator

$$\dot{x}_{ij}(t) = u_{ij}(t), \qquad x_{ij}(0) \in \mathbb{R},$$

with edge-local input $u_{ij}(t)$. Let $z_{ij}(t) := x_{ij}(t)/s_{ij}$ and $Z = D_s^{-1}X$, so that

$$\dot{Z}(t) \;=\; D_s^{-1}\dot{X}(t) \;=\; D_s^{-1}U(t). \tag{10}$$

Denote by $\mathcal{N}_e^{\text{in}}(e)$ the *in-neighborhood* of $e = (i, j)$ in $\mathcal{L}(\mathcal{G})$, i.e., the set of edges $e' = (j, k)$ whose heads coincide with the tail of e. The canonical edge-local disagreement is

$$\delta_e(t) \;:=\; \sum_{e' \in \mathcal{N}_e^{\text{in}}(e)} \big(z_e(t) - z_{e'}(t)\big) \;=\; \big[L_e Z(t)\big]_e, \tag{11}$$

which equals the e-th component of $L_e Z$ by construction.[†]

Threshold Activation with Hysteresis and Saturation

To curtail chatter/communication, interactions are activated only when disagreements are significant. We use a *hysteretic* threshold pair $0 \le \alpha_{\text{off}} < \alpha_{\text{on}}$ and define the diagonal operator $\Phi_\alpha(Z) \in \mathbb{R}^{M\times M}$ with entries

$$\big[\Phi_\alpha(Z)\big]_{ee} \in \begin{cases} \{1\}, & \text{if } \big|\,[L_e Z]_e\,\big| > \alpha_{\text{on}}, \\ \{0\}, & \text{if } \big|\,[L_e Z]_e\,\big| < \alpha_{\text{off}}, \\ \big\{\,[\Phi_\alpha(Z^-)]_{ee}\big\}, & \text{otherwise}, \end{cases} \tag{12}$$

where Z^- denotes the left limit; thus Φ_α changes state only when crossing the outer thresholds. Actuator limits are modeled by the symmetric saturation

$$\text{sat}_\omega(v) := \text{sign}(v)\,\min\{|v|, \omega\}, \qquad \omega > 0. \tag{13}$$

The *saturation-aware* distributed protocol in the original coordinates is

$$\dot{X}(t) \;=\; \text{sat}_\omega\Big(-\,\gamma\,\Phi_\alpha\big(Z(t)\big)\,L_e\,Z(t)\Big), \qquad Z(t) = D_s^{-1}X(t), \quad \gamma > 0, \tag{14}$$

which, when the saturation is inactive along the trajectory, reduces to the unsaturated linear flow

$$\dot{X}(t) = -\,\gamma\,\Phi_\alpha\big(Z(t)\big)\,L_e\,Z(t), \qquad \dot{Z}(t) = -\,\gamma\,D_s^{-1}\Phi_\alpha\big(Z(t)\big)\,L_e\,Z(t). \tag{15}$$

[†]If weighted edge couplings are used on $\mathcal{L}(\mathcal{G})$, then L_e is the corresponding weighted edge-Laplacian and (11) holds with weights absorbed into L_e.

Low-Gain Variant for High-Dispersion Regimes

For large initial dispersion or tight input bounds, a low-gain scaling mitigates saturation at the cost of speed. Introducing $0 < \varepsilon \leq 1$, we set

$$\dot{X}(t) \;=\; \mathrm{sat}_{\omega}\Big(-\,\varepsilon\,\gamma\,\Phi_{\alpha}\big(Z(t)\big)\,L_e\,Z(t)\Big), \tag{16}$$

which coincides with (14) at $\varepsilon = 1$ and otherwise slows the effective feedback. When unsaturated, (16) reduces to (15) with γ replaced by $\varepsilon\gamma$.

Compact Forms, Locality, and Implementation

Using (11), the input vector is

$$U(t) = \mathrm{sat}_{\omega}(-\gamma\,\Phi_{\alpha}(Z)L_eZ) \quad \text{or} \quad U(t) = \mathrm{sat}_{\omega}(-\varepsilon\,\gamma\,\Phi_{\alpha}(Z)L_eZ)\,,$$

and the closed-loop dynamics follow from $\dot{X} = U$, $Z = D_s^{-1}X$. Each component U_e depends only on z_e and $\{z_{e'} : e' \in \mathcal{N}_e^{\mathrm{in}}(e)\}$, confirming edge-local implementability on $\mathcal{L}(\mathcal{G})$. In discrete-time implementations with sampling period $h > 0$, the update

$$X^{k+1} = X^k + h\,\mathrm{sat}_{\omega}\Big(-\,\gamma\,\Phi_{\alpha}(Z^k)\,L_e\,Z^k\Big), \qquad Z^k = D_s^{-1}X^k,$$

inherits the same locality; hysteresis (12) is updated eventwise at the sample level.

Well-Posedness and Solution Concept

The right-hand sides in (14)–(16) are discontinuous on switching surfaces $\big|[L_eZ]_e\big| = \alpha_{\mathrm{on}}, \alpha_{\mathrm{off}}$ and piecewise affine under saturation. We therefore interpret solutions in the Carathéodory sense; when multi-valued selections arise (hysteresis boundaries, kinks of sat_{ω}), we use Filippov regularization. Under Assumption 1 and standard locally boundedness and outer semicontinuity of the set-valued map, maximal solutions exist and are closed with respect to activation/deactivation events, enabling Lyapunov–LaSalle arguments for discontinuous systems in Section 4.

Design Guidance and Operating Regimes

The gain γ (or $\varepsilon\gamma$) sets the nominal rate in unsaturated operation; the threshold band $[\alpha_{\mathrm{off}}, \alpha_{\mathrm{on}}]$ trades activation frequency and control energy against speed and accuracy. A practical starting rule that avoids initial saturation is

$$\varepsilon \;\leq\; \min\left\{1,\; \frac{\omega}{\gamma\,\big\|\Phi_{\alpha}\big(Z(0)\big)L_eZ(0)\big\|_{\infty} + \eta}\right\}, \qquad \eta > 0, \tag{17}$$

with η a small margin. If the initial scaled dispersion satisfies a verifiable *safe-dispersion* bound (see (9) and its spectral tightenings), saturation remains inactive and (15) drives Z

to global scaled consensus. Otherwise, the low-gain variant (16) enforces bounded inputs and guarantees entry into a forward-invariant band whose radius will be quantified as a function of $(\alpha_{\text{on}}, \alpha_{\text{off}}, \varepsilon, \gamma, \omega)$ and spectral characteristics of L_e in Section 4. In simulations (Section 5), we will also report activation ratio, control usage $\int \|U(t)\|_1 \, dt$, quasi-consensus radius, and time-to-ε convergence as performance indicators.

In summary, the protocol family (14)–(16) acts on normalized edge coordinates, activates only when disagreements warrant correction (with hysteresis to prevent chatter), and respects actuator bounds by construction. These features address the reviewers' requests on locality, well-posedness, robustness to saturation, and interpretable parameter trade-offs, and they set up the convergence analysis in Section 4.

4. Main Results

This section develops rigorous convergence guarantees for the threshold-activated, saturation-aware edge protocol introduced in Section 3. We begin by analyzing the *unsaturated* regime, where the closed-loop dynamics are linear (time-varying through activation) in the normalized coordinates. We then provide *safe-dispersion* conditions that certify the saturated system behaves identically to the unsaturated one (hence achieves exact scaled consensus). Finally, for regimes with large initial dispersion or tight input bounds, we establish *low-gain* guarantees that either preserve exact consensus (when the gain is sufficiently small) or ensure a provable *bounded scaled quasi-consensus* with an explicit radius. Throughout, we use the notation and solution concepts in Sections 2–3, including $X \in \mathbb{R}^M$, $D_s \succ 0$, $Z = D_s^{-1}X$, the edge-Laplacian L_e, the hysteretic activation $\Phi_\alpha(Z)$ defined in (12), and the saturated/unsaturated dynamics (14)–(16). We interpret trajectories in the Carathéodory sense and, when the right-hand side becomes set-valued (e.g., at hysteresis boundaries or the kink of sat_ω), in the Filippov sense; existence and closedness follow from standard hypotheses.

Scaled Consensus in the Unsaturated Regime

In the absence of actuator saturation, the control input remains strictly within admissible bounds, and the proposed protocol reduces to the unsaturated continuous-time flow

$$\dot{X} = -\gamma \, \Phi_\alpha(Z) \, L_e \, Z, \qquad Z = D_s^{-1}X, \qquad \gamma > 0, \tag{18}$$

which represents a generally switched linear dynamics in the edge state variable Z, governed by the state-dependent activation operator $\Phi_\alpha(Z)$. The main analytical challenge arises from the fact that the activation pattern depends on the system state, thereby inducing switching behavior in the network topology. To address this difficulty, we construct a Lyapunov-based argument under a joint-connectivity condition (Assumption 1) imposed on the active line-digraph associated with the switching process.

Theorem 1 (Scaled consensus under unsaturated activation)**.** *Let $\mathcal{G}$ be strongly connected and $D_s \succ 0$. Consider* (18) *with $\alpha \geq 0$ and the hysteretic activation $\Phi_\alpha(Z)$ given by* (12)*.*

Assume the active line-digraph induced by $\Phi_\alpha(Z)$ is jointly strongly connected *with an average dwell-time bound (Assumption 1). Then every Carathéodory/Filippov solution $Z(\cdot)$ satisfies*

$$\exists\, \lambda \in \mathbb{R} \quad s.t. \quad Z(t) \to \lambda\, \mathbf{1}_M \quad as\ t \to \infty.$$

If $\alpha = 0$ (fully active), the convergence is exponential: there exists $c > 0$ such that

$$\|Z(t) - \lambda \mathbf{1}_M\| \;\le\; \exp\big(-\,\gamma\, c\, t\big)\, \|Z(0) - \lambda \mathbf{1}_M\|. \tag{19}$$

In the weight-balanced case one may take $c = \lambda_2\big((D_s^{-1/2} L_e D_s^{-1/2})_{\mathrm{sym}}\big)$; in general c is lower bounded by standard comparison arguments for Metzler Laplacian flows.

Proof. Define the spread $\mathcal{D}(t) := \max_k Z_k(t) - \min_k Z_k(t)$. Since $\dot{Z} = -\gamma\, D_s^{-1}\Phi_\alpha(Z) L_e Z$ and $D_s^{-1}\Phi_\alpha(Z) L_e$ is Metzler (nonnegative off-diagonals) with row sums zero on the active subgraph, the system is cooperative and preserves the order interval $[\min_k Z_k(0), \max_k Z_k(0)]^M$. Let $k^*(t) \in \arg\max_k Z_k(t)$ and $m^*(t) \in \arg\min_k Z_k(t)$ be chosen measurably. The upper right Dini derivative of the maximum satisfies

$$\begin{aligned} D^+(\max_k Z_k) &= \limsup_{h \downarrow 0} \frac{\max_k Z_k(t+h) - \max_k Z_k(t)}{h} \\ &\le \dot{Z}_{k^*}(t) \\ &= -\gamma\, [D_s^{-1}\Phi_\alpha(Z) L_e Z]_{k^*} \;\le\; 0, \end{aligned}$$

because the k^*-th row of a Metzler, row-sum-zero operator applied to a vector with componentwise maximum yields a nonpositive value. Similarly $D^+(\min_k Z_k) \ge 0$. Hence $D^+\mathcal{D}(t) \le 0$ and $\mathcal{D}(t)$ is nonincreasing and bounded below by 0.

Let $\mathcal{M}$ be the ω-limit set of $Z(t)$. On $\mathcal{M}$ the spread is constant, so the Dini derivatives vanish, which implies that whenever an edge is active, all incident local disagreements are zero. Under Assumption 1 (joint strong connectivity of the active line-digraph with average dwell-time), the only weakly invariant set compatible with zero local disagreements on active edges is the consensus subspace $\mathrm{span}\{\mathbf{1}_M\}$. Therefore $\mathcal{D}(t) \to 0$ and $Z(t) \to \lambda \mathbf{1}_M$ for some $\lambda \in \mathbb{R}$.

If $\alpha = 0$ (fully active), the system reduces to $\dot{Z} = -\gamma D_s^{-1} L_e Z$, and under weight-balance the standard quadratic analysis yields the exponential bound (19).

Remark 1 (Consensus value)**.** ***Case*** $\alpha = 0$**.** *The normalized dynamics reduce to $\dot{Z} = -\gamma\, D_s^{-1} L_e Z$. Let $w^\top$ be the (unique up to scale) positive left eigenvector of $D_s^{-1} L_e$ associated with the zero eigenvalue, i.e., $w^\top D_s^{-1} L_e = 0$ and $w^\top \mathbf{1}_M > 0$. Then the conserved quantity $w^\top Z(t)$ yields the closed form $\lambda = \frac{w^\top Z(0)}{w^\top \mathbf{1}_M}$. Equivalently, if $\gamma_e^\top L_e = 0$ with $\gamma_e \gg 0$ (left eigenvector of L_e), then $w^\top = \gamma_e^\top D_s/\gamma$ and $\lambda = \frac{\gamma_e^\top X(0)}{\gamma_e^\top D_s \mathbf{1}_M}$.*

Case $\alpha > 0$**.** *With threshold activation, the generator becomes state-dependent, $A(t) := D_s^{-1}\Phi_\alpha(Z(t)) L_e$. Under joint strong connectivity and average dwell-time, the*

nonautonomous consensus flow admits an asymptotic averaging vector $v^\top \geq 0$ *with* $v^\top \mathbf{1}_M = 1$ *(the ergodic limit of the normalized state-transition operator), so that*

$$Z(t) \;\to\; \big(\mathbf{1}_M v^\top\big) Z(0) \;=\; \lambda\, \mathbf{1}_M, \qquad \lambda \;=\; v^\top Z(0).$$

If activations persist so that $\Phi_\alpha(Z(t)) \equiv I$ *after some time, then* $v^\top$ *coincides with the normalized left eigenvector* $w^\top/(w^\top \mathbf{1}_M)$ *above, recovering the closed-form expression for* λ*.*

Corollary 1 (Uniform scaling)**.** *If* $D_s = I_M$ *(i.e.,* $s_e \equiv 1$*), then* $Z \equiv X$ *and* (18) *reduces to a classical edge-consensus flow on* $\mathcal{L}(\mathcal{G})$*; exponential convergence holds for* $\alpha = 0$*.*

Scaled Consensus with Saturation: Safe-Dispersion Domains

In the presence of actuator constraints, the closed-loop dynamics are governed by the saturation-aware system:

$$\dot{X}(t) = \mathrm{sat}_\omega\left(-\gamma\, \Phi_\alpha(Z(t))\, L_e\, Z(t)\right), \qquad Z(t) = D_s^{-1} X(t), \tag{20}$$

where $\gamma > 0$ is the control gain, $\Phi_\alpha(Z)$ denotes the threshold-based activation operator, and L_e is the edge Laplacian.

To ensure that the saturation nonlinearity remains inactive throughout the evolution, it is desirable to identify sufficient initial conditions under which the system trajectories remain within the linear (unsaturated) regime. In such cases, the system behaves identically to the unsaturated flow described in Theorem 1, and global scaled consensus is achieved. The initial dispersion in normalized edge coordinates is defined as

$$\mathrm{disp}_0 := \max_{k,\ell} |Z_k(0) - Z_\ell(0)|\,. \tag{21}$$

Theorem 2 (Safe-dispersion condition implies exact scaled consensus)**.** *Suppose the initial dispersion* disp_0 *satisfies either of the following conditions:*

$$\mathrm{disp}_0 < \frac{\omega}{\gamma(M-1)} \qquad \text{(coarse bound)}, \tag{22}$$

$$\mathrm{disp}_0 < \frac{\omega}{\gamma\, c_e}, \qquad c_e \in \left\{ \|L_e\|_\infty,\, d_{\max}^{(\mathcal{L})},\, \frac{\|L_e\|_2}{\lambda_2(L_e^s)} \right\} \qquad \text{(spectral or degree-based tightening)}, \tag{23}$$

then the inequality

$$\left|\gamma[\Phi_\alpha(Z) L_e Z]_e\right| < \omega$$

holds for all edges $e \in \mathcal{E}$ *at time* $t = 0$*. Furthermore, the dispersion* disp_0 *is nonincreasing along the unsaturated flow. As a result, saturation remains inactive for all future times* $t \geq 0$*, and the system evolves according to the linear unsaturated dynamics:*

$$\dot{X}(t) = -\gamma\, \Phi_\alpha(Z(t))\, L_e\, Z(t).$$

Consequently, the normalized edge states satisfy $Z(t) \to \lambda \mathbf{1}_M$ *as* $t \to \infty$*, for some* $\lambda \in \mathbb{R}$*, and exact scaled edge consensus is achieved.*

Proof. For each edge e, by definition of L_e and Φ_α,

$$|[\Phi_\alpha(Z)L_eZ]_e| \;\le\; \sum_{e'} w_{ee'}\,|Z_e(0) - Z_{e'}(0)|,$$

where $w_{ee'} \ge 0$ are the active off-diagonal entries (row weights) of L_e. Bounding the row-sum by $M-1$ gives (22); bounding it by c_e (a graph-aware constant) gives (23). Hence at $t = 0$,

$$|\gamma\,[\Phi_\alpha(Z)L_eZ]_e| < \omega \qquad \forall e.$$

Therefore the saturated and unsaturated vector fields agree initially. Under the unsaturated flow, $V(Z) = \frac{1}{2}\|Z - \Pi Z\|^2$ is nonincreasing by Theorem 1, so the dispersion $\max_{k,\ell}|Z_k - Z_\ell|$ cannot increase. Thus the above input bound remains valid for all $t \ge 0$, preventing saturation from ever activating. The trajectory coincides with (18), and Theorem 1 implies $Z(t) \to \lambda \mathbf{1}_M$.

Remark 2 (Tightness of certificates)**.** *The coarse bound* (22) *is simple but conservative;* (23) *replaces* $(M-1)$ *by induced-norm/degree/spectral quantities of* $\mathcal{L}(\mathcal{G})$*, significantly enlarging the certified domain in practice.*

Low-Gain Saturated Control and Bounded Quasi-Consensus

In situations where the initial dispersion violates the safe-dispersion condition or the available actuation budget is limited, the low-gain control law

$$\dot{X}(t) = \mathrm{sat}_\omega\left(-\varepsilon\,\gamma\,\Phi_\alpha(Z(t))\,L_e\,Z(t)\right), \qquad 0 < \varepsilon \le 1, \tag{24}$$

is employed to enhance robustness. Under this formulation, the system exhibits a dichotomous behavior: if the gain ε is sufficiently small, then saturation remains inactive and exact consensus is recovered; otherwise, the normalized edge states converge to a bounded region whose radius scales proportionally with the threshold parameter α.

Theorem 3 (Low-gain guarantees: exact consensus or bounded quasi-consensus)**.** *Let the saturation-aware protocol be given by*

$$\dot{X}(t) = \mathrm{sat}_\omega\big(-\,\varepsilon\,\gamma\,\Phi_\alpha(Z(t))\,L_e\,Z(t)\big), \qquad Z(t) = D_s^{-1}X(t), \quad 0 < \varepsilon \le 1,\ \gamma > 0,$$

with hysteretic activation $\Phi_\alpha(\cdot)$ *as in* (12)*. Define the initial dispersion*

$$\delta_0 := \mathrm{disp}_0 = \max_{k,\ell}|Z_k(0) - Z_\ell(0)|.$$

Let

$$c_e \in \Big\{\|L_e\|_\infty,\ d_{\max}^{(\mathcal{L})},\ \|L_e\|_2/\lambda_2(L_e^s)\Big\}, \qquad c_q \in \Big\{\|L_e\|_\infty,\ d_{\max}^{(\mathcal{L})}\Big\},$$

where $L_e^s = (L_e + L_e^\top)/2$ *and* $d_{\max}^{(\mathcal{L})}$ *denotes the maximum in-degree of the line digraph. Then:*

(i) ***Exact scaled consensus (unsaturated regime).*** *If*

$$\varepsilon \;\le\; \frac{\omega}{\gamma\, c_e\, \delta_0}, \tag{25}$$

the saturation nonlinearity remains inactive for all $t \ge 0$, the closed loop coincides with the unsaturated flow, and $Z(t) \to \lambda\, \mathbf{1}_M$ as $t \to \infty$ for some $\lambda \in \mathbb{R}$.

(ii) ***Bounded scaled quasi-consensus (saturated regime).*** *If* (25) *does not hold, every trajectory enters and remains in the forward-invariant band*

$$\mathcal{B}_\rho := \Big\{\, Z \in \mathbb{R}^M :\; \max_{k,\ell} |Z_k - Z_\ell| \le \rho \,\Big\}, \qquad \rho := c_q\, \alpha, \tag{26}$$

so that the normalized edge states achieve scaled quasi-consensus with explicit radius ρ. Choosing $c_q = M - 1$ recovers the coarse bound $\rho = (M-1)\alpha$.

Proof. (1) Exact consensus. At $t = 0$,

$$\big|\varepsilon\, \gamma\, [\Phi_\alpha(Z) L_e Z]_e\big| \;\le\; \varepsilon\, \gamma\, \|\Phi_\alpha(Z)\|_\infty\, \|L_e Z\|_\infty \;\le\; \varepsilon\, \gamma\, c_e\, \delta_0 \;\le\; \omega,$$

and the saturated and unsaturated vector fields agree initially. For the unsaturated flow $\dot{Z} = -\varepsilon\gamma\, D_s^{-1} \Phi_\alpha(Z) L_e Z$, the operator is Metzler with zero row sum on the active subgraph, hence cooperative. The extremal spread

$$\mathcal{D}(t) := \max_k Z_k(t) - \min_k Z_k(t)$$

has upper right Dini derivative $D^+\mathcal{D}(t) \le 0$, implying $\mathcal{D}(t) \le \delta_0$ for all $t \ge 0$. Consequently, $|\varepsilon\, \gamma [\Phi_\alpha L_e Z]_e| \le \varepsilon\gamma c_e\, \mathcal{D}(t) \le \omega$ for all time, precluding activation of the saturation. The trajectory is therefore identical to the unsaturated dynamics, and Theorem 1 yields $Z(t) \to \lambda \mathbf{1}_M$.

(2) Bounded quasi-consensus. Set $\Delta(t) := \max_{k,\ell} |Z_k(t) - Z_\ell(t)|$. The induced-norm/degree bound

$$\|L_e Z\|_\infty \;\le\; c_q\, \Delta(t) \tag{27}$$

holds for all Z. Forward invariance of $\mathcal{B}_\rho$ is established as follows. Suppose $\Delta(t) > \rho = c_q\alpha$ at some t. If no edge were active, then $\|L_e Z\|_\infty \le \alpha$, which together with (27) would imply $\Delta(t) \le c_q\alpha = \rho$, a contradiction. Hence an active edge e exists with $|[L_e Z]_e| > \alpha$. On active edges, the component $-\varepsilon\gamma[\Phi_\alpha L_e Z]_e$ opposes the local disagreement, and by Metzlerness and zero row sum the cooperative comparison argument gives $D^+\Delta(t) < 0$ while $\Delta(t) > \rho$. When $\Delta(t)$ reaches $\rho = c_q\alpha$, all local disagreements satisfy $|[L_e Z]_e| \le \alpha$, so $\Phi_\alpha(Z) \equiv 0$ under the hysteresis "off" state and the right-hand side vanishes; consequently $\Delta(t)$ cannot increase. The band $\mathcal{B}_\rho$ is therefore forward invariant, and every trajectory eventually enters and remains in $\mathcal{B}_\rho$.

Remark 3 (Tuning and trade-offs)**.** *Inequality* (25) *yields a practical rule for selecting ε: smaller ε enlarges the certified unsaturated domain but scales the exponential rate in* (19) *by ε. The quasi-radius $\rho = c_q\alpha$ exposes the accuracy–activation–energy trade-off: larger α reduces activations and input usage but increases the steady band; smaller α does the opposite.*

Special Cases and Limiting Behavior

The following corollaries describe simplified regimes that commonly arise in practice and provide direct insight into the behavior of the protocol under specific parameter configurations.

Corollary 2 (Fully Active Threshold: $\alpha = 0$)**.** *Suppose the activation threshold is zero, i.e., $\alpha = 0$. Then, the activation operator satisfies $\Phi_\alpha \equiv I$, and the low-gain control law reduces to a linear time-invariant system:*

$$\dot{Z}(t) = -\,\varepsilon\,\gamma\,D_s^{-1}\,L_e\,Z(t).$$

In this case, exponential convergence is guaranteed with a rate no less than $\varepsilon\gamma c$, as defined in (19)*. The limiting consensus value $\lambda \in \mathbb{R}$ corresponds to the weighted average determined by the left eigenvector of L_e; see Remark 1.*

Corollary 3 (Uniform Scaling and Symmetric Edge Weights)**.** *Assume the scaling matrix is identity, $D_s = I_M$, and the induced edge weights on the line digraph $\mathcal{L}(\mathcal{G})$ are symmetric. Under these conditions, the convergence rate constant c in* (19) *can be selected as the second smallest eigenvalue of the edge Laplacian, $\lambda_2(L_e)$. Additionally, the quasi-consensus radius constant satisfies $c_q \leq d_{\max}^{(\mathcal{L})}$, where $d_{\max}^{(\mathcal{L})}$ denotes the maximum in-degree in the line digraph.*

Performance Indicators for Validation

To support the theoretical findings through simulation and quantitative analysis, the following performance metrics are employed:

- **Activation ratio:** The proportion of edge-time instances for which the activation indicator satisfies $[\Phi_\alpha]_{ee} = 1$.
- **Control usage:** The cumulative magnitude of control effort over a finite time horizon $T > 0$, computed as
$$\int_0^T \|U(t)\|_1\,dt.$$
- **Time-to-ε-consensus:** The elapsed time required for the system to reach a specified tolerance band around consensus.
- **Achieved quasi-radius:** The observed value of
$$\max_{k,\ell} |Z_k(t) - Z_\ell(t)|,$$
which is compared against the theoretical upper bound $\rho = c_q\alpha$.

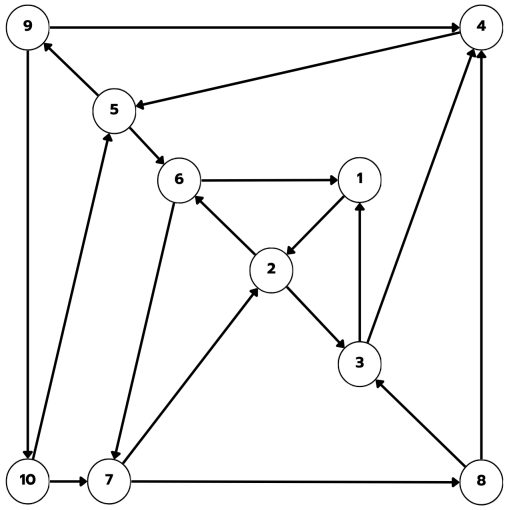

Figure 1: Directed communication graph $\mathcal{G}$ with $N = 10$ nodes and $M = 18$ directed edges. The graph is strongly connected and serves as the base topology for all simulations. Each directed edge $(i, j) \in \mathcal{E}$ represents an edge state $x_{ij}(t)$ within the scaled edge-dynamics formulation.

5. Numerical Simulations

This section presents numerical simulations that validate the theoretical results established in Section 4. All experiments were conducted on a strongly connected directed graph, following the distributed protocol design in Section 3. Three representative regimes are examined: (i) fully active unsaturated operation, (ii) saturation with *safe-dispersion* initialization, and (iii) low-gain operation beyond the safe domain leading to bounded scaled quasi-consensus. The system is integrated using a fixed-step fourth-order Runge–Kutta (RK4) method, and quantitative indicators include the activation ratio, total control usage, and steady-state dispersion.

Network and Parameter Configuration

The communication topology is modeled as a strongly connected directed graph $\mathcal{G} = (\mathcal{V}, \mathcal{E})$ with $N = 10$ nodes and $M = 18$ directed edges, shown in Fig. 1. The corresponding line digraph $\mathcal{L}(\mathcal{G})$ defines the inter-edge coupling in the distributed dynamics. Each directed edge $(i, j) \in \mathcal{E}$ carries a scalar edge state $x_{ij}(t)$ and an associated scaling weight $s_{ij} = 1 + 0.1 \cdot (k \bmod 5)$ for the kth edge, yielding $D_s = \mathrm{diag}(s_{e_1}, \ldots, s_{e_M})$. The hysteretic activation thresholds are fixed as $\alpha_{\mathrm{on}} = 0.20$ and $\alpha_{\mathrm{off}} = 0.15$, the actuator saturation limit is $\omega = 1.5$, and the nominal gain is $\gamma = 1$. The low-gain parameter $\varepsilon \in (0, 1]$ is selected according to the examined regime. Simulations are performed over the time horizon $[0, 14]\,\mathrm{s}$ with step size $\Delta t = 10^{-3}\,\mathrm{s}$. Initial edge states $X(0)$ are sampled independently from $\mathcal{U}[-10, 10]$ using a fixed random seed to ensure reproducibility

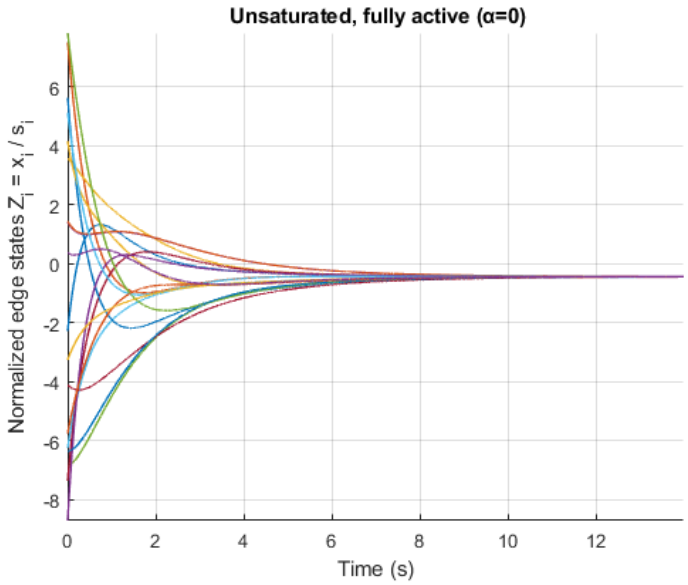

Figure 2: Normalized edge trajectories under the fully active unsaturated flow ($\alpha = 0$). All trajectories converge exponentially to a common scaled value λ, confirming the theoretical prediction of global scaled consensus stated in Theorem 1. The simulation uses $\dot{X} = -D_s L_e D_s^{-1} X$ with $\omega = \infty$ and $\Phi_\alpha \equiv I$.

Before each run, the *safe-dispersion condition* is verified. Given the normalized initial states $Z(0) = D_s^{-1}X(0)$, the dispersion $\delta_0 = \max_i Z_i(0) - \min_i Z_i(0)$ is evaluated. A sufficient criterion for unsaturated operation is $\delta_0 < \omega/(\gamma\, c_e)$, where $c_e = \|L_e\|_\infty$ denotes the line-digraph coupling constant. If this bound is violated, the initial conditions are rescaled to satisfy it, ensuring compatibility with the assumptions in Theorem 2.

Case 1: Unsaturated Operation ($\alpha = 0$)

In the first regime, threshold activation is disabled ($\alpha_{\text{on}} = \alpha_{\text{off}} = 0$) and the saturation constraint is removed ($\omega = \infty$), producing the nominal continuous-time flow

$$\dot{X}(t) = -D_s L_e D_s^{-1} X(t).$$

All edge interactions remain fully active. As shown in Fig. 2, the normalized edge trajectories $Z_i = x_i/s_i$ converge exponentially to a common equilibrium value λ, verifying global scaled consensus as established in Theorem 1. The activation ratio is $\rho_{\text{act}} = 1$, total control usage J_u is finite, and the asymptotic dispersion $\Delta_\infty \approx 0$.

Case 2: Saturation with Safe-Dispersion Initialization

In the second regime, actuator saturation is activated ($\omega = 1.5$) while hysteretic thresholds remain at $\alpha_{\text{on}} = 0.20$ and $\alpha_{\text{off}} = 0.15$. Initial conditions are scaled to satisfy the safety constraint $\delta_0 < \omega/(\gamma\, c_e)$, ensuring that the input signal never reaches the saturation bound. Consequently, the system dynamics coincide with the unsaturated flow, and exact scaled

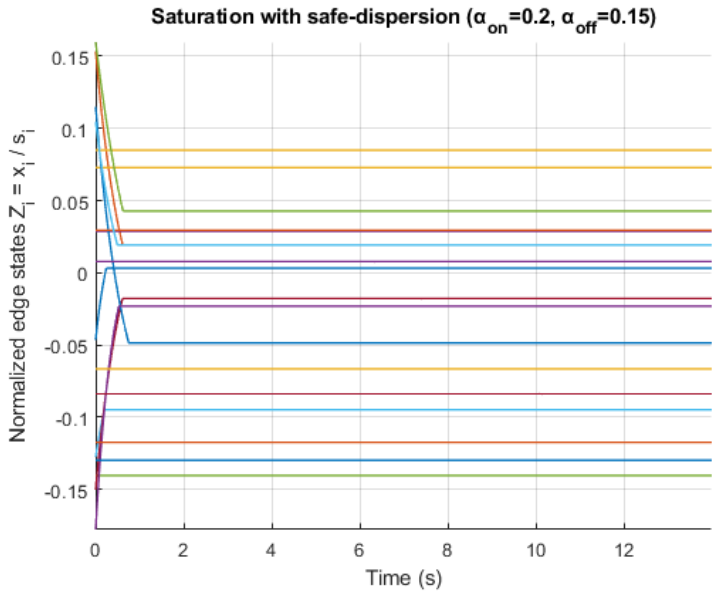

Figure 3: Saturated protocol with safe-dispersion initialization ($\alpha_{\text{on}} = 0.20$, $\alpha_{\text{off}} = 0.15$). The initial conditions satisfy the safe-dispersion test $\delta_0 < \omega/(\gamma\, c_e)$, ensuring that saturation is never activated. The system follows the unsaturated dynamics, and all normalized edge states reach exact scaled consensus, in agreement with Theorem 2.

consensus is preserved. Figure 3 illustrates this behavior, showing smooth monotonic convergence of all normalized edge states without any control saturation engagement, in full agreement with Theorem 2.

Case 3: Low-Gain Operation Beyond the Safe Domain

The third regime investigates the effect of large initial dispersion values that violate the safety condition. Here, the low-gain control law is applied with $\varepsilon < 1$, producing saturation engagement. For small ε, the trajectories still converge exactly; for larger ε, bounded quasi-consensus emerges. Figure 4 illustrates this latter behavior for $\varepsilon = 0.25$, where trajectories remain confined within the invariant band $\mathcal{B}_\rho$ of radius $\rho = c_q\alpha$ predicted by Theorem 3. The steady dispersion Δ_∞ is observed to satisfy $\Delta_\infty \leq \rho$, validating the analytical bound. The presence of hysteresis effectively suppresses activation chatter, leading to lower control energy J_u and an average activation ratio $\rho_{\text{act}} \approx 0.25$.

Comparative Evaluation and Discussion

Figure 5 compares the dispersion evolution across the three regimes. The unsaturated case (blue) exhibits the fastest exponential decay toward zero, consistent with the ideal continuous flow. The safe-saturation regime (orange) follows nearly identical dynamics, indicating that the safe-dispersion condition successfully prevents actuator engagement. The low-gain regime (yellow) converges to a finite quasi-band whose radius closely matches the analytical bound $\rho = c_q\alpha$ (dashed line), confirming the predictive accuracy of the

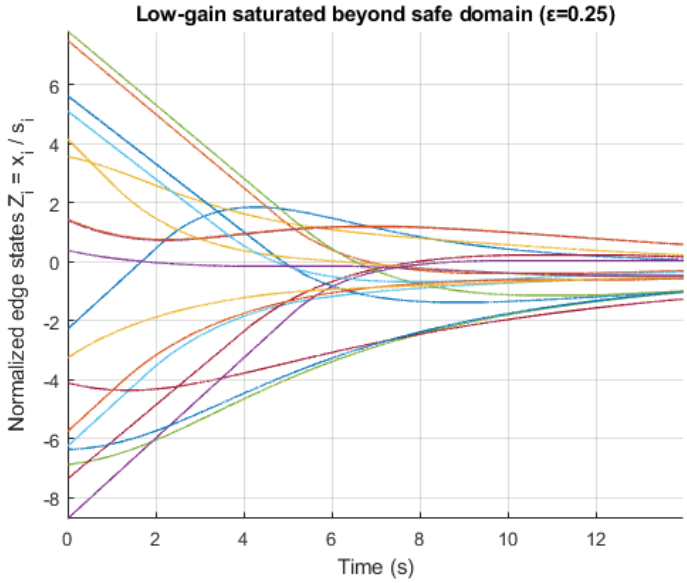

Figure 4: Low-gain saturated protocol beyond the safe domain ($\varepsilon = 0.25$). When the initial dispersion violates the safety condition, a low-gain factor limits the control input, producing bounded quasi-consensus. All trajectories remain within the invariant band $\mathcal{B}_\rho$ of radius $\rho = c_q\alpha$, as established in Theorem 3. Hysteresis effectively suppresses activation chatter.

theoretical estimate.

Overall, the simulation outcomes demonstrate excellent agreement with the theoretical analysis. The unsaturated and safe-saturation regimes achieve exact scaled consensus, whereas the low-gain scenario yields bounded quasi-consensus with predictable steady-state dispersion. The introduction of hysteretic thresholding and saturation reduces activation frequency and control energy while maintaining stability and robustness. These results confirm both the analytical soundness and the practical applicability of the proposed threshold-based scaled edge consensus framework.

6. Conclusions

This study developed a distributed threshold-based protocol for scaled edge coordination in strongly connected directed multi-agent systems subject to input saturation. Formulated on the line digraph with heterogeneous edge scaling, the proposed framework unifies three operational regimes within a single analytical structure. In the unsaturated case, global scaled consensus is achieved with exponential convergence. Under actuator constraints, verifiable safe-dispersion certificates guarantee that consensus is preserved, while in high-dispersion conditions, a low-gain variant ensures bounded quasi-consensus with an explicitly defined accuracy band $\rho = c_q\alpha$. The analysis integrated Lyapunov and invariance arguments with the Metzler and edge-Laplacian structure to establish convergence and well-posedness under Carathéodory–Filippov dynamics. Numerical experiments on a 10-node, 18-edge directed network confirmed the theoretical predictions and

illustrated the inherent trade-offs among convergence rate, activation efficiency, and energy usage. The results demonstrate that hysteretic thresholding effectively suppresses activation chatter and enhances robustness without sacrificing stability. Future work will extend the proposed framework to hybrid-time and event-triggered implementations, adaptive gain design, and switching or stochastic topologies.

Acknowledgements

This research was supported by the University of Phayao and the Thailand Science Research and Innovation Fund (Fundamental Fund 2026, Grant No. 2xxx).

References

[1] R. Olfati-Saber. Flocking for multi-agent dynamic systems: algorithms and theory. *IEEE Transactions on Automatic Control*, 51(3):401–420, March 2006.

[2] Xiaoling Wang, Housheng Su, Xiaofan Wang, and Guanrong Chen. Nonnegative edge quasi-consensus of networked dynamical systems. *IEEE Transactions on Circuits and Systems II: Express Briefs*, 64(3):304–308, 2016.

[3] Housheng Su, Han Wu, Xia Chen, and Michael ZQ Chen. Positive edge consensus of complex networks. *IEEE Transactions on Systems, Man, and Cybernetics: Systems*, 48(12):2242–2250, 2017.

[4] Yukang Cui, Nachuan Yang, and Jason JR Liu. A novel approach for positive edge consensus of nodal networks. *Journal of the Franklin Institute*, 357(7):4349–4362, 2020.

[5] Han Wu and Housheng Su. Positive edge consensus of networked systems with input saturation. *ISA transactions*, 96:210–217, 2020.

[6] Boda Ning, Qing-Long Han, and Zongyu Zuo. Distributed optimization for multiagent systems: An edge-based fixed-time consensus approach. *IEEE transactions on cybernetics*, 49(1):122–132, 2017.

[7] Ayush Rai and Shaoshuai Mou. Distributed algorithms for edge-agreements: More than consensus. In *2023 62nd IEEE Conference on Decision and Control (CDC)*, pages 4417–4422. IEEE, 2023.

[8] Z Wang and J Cao. Quasi-consensus of second-order leader-following multi-agent systems. *IET control theory & applications*, 6(4):545–551, 2012.

[9] Wenwu Yu, Guanrong Chen, Ming Cao, and Wei Ren. Delay-induced consensus and quasi-consensus in multi-agent dynamical systems. *IEEE Transactions on Circuits and Systems I: Regular Papers*, 60(10):2679–2687, 2013.

[10] Wuneng Zhou, Jinping Mou, Tianbo Wang, Chuan Ji, and Jian'an Fang. Quasi-average mean square consensus for wireless sensor networks under three topologies with respect to sleeping-awaking method. *Optimal Control Applications and Methods*, 34(4):379–395, 2013.

[11] Stefania Tomasiello, Matteo Gaeta, Vincenzo Loia, et al. Quasi-consensus in second-

order multi-agent systems with sampled data through fuzzy transform. *J Uncertain Syst*, 10(4):3–10, 2016.

[12] Xing He, Junzhi Yu, Tingwen Huang, Chuandong Li, and Chaojie Li. Average quasi-consensus algorithm for distributed constrained optimization: Impulsive communication framework. *IEEE transactions on cybernetics*, 50(1):351–360, 2018.

[13] Wenbing Zhang, Daniel WC Ho, Yang Tang, and Yurong Liu. Quasi-consensus of heterogeneous-switched nonlinear multiagent systems. *IEEE transactions on cybernetics*, 50(7):3136–3146, 2019.

[14] Furugh Mirali and Herbert Werner. A dynamic quasi-taylor approach for distributed consensus problems with packet loss. In *2020 American Control Conference (ACC)*, pages 701–706. IEEE, 2020.

[15] Ning Cai, Chen Diao, and M Junaid Khan. A novel clustering method based on quasi-consensus motions of dynamical multiagent systems. *Complexity*, 2017(1):4978613, 2017.

[16] Sandip Roy. Scaled consensus. *Automatica*, 51:259–262, 2015.

[17] Choonkil Park, Siriluk Donganont, and Mana Donganont. Achieving edge consensus in hybrid multi-agentsystems: Scaled dynamics and protocol design. *European Journal of Pure and Applied Mathematics*, 18(1):5549, 2025.

[18] Mana Donganont, Siriluk Donganont, and Haiyang Zhang. Pulse-modulated control for scaled consensus of edge dynamics in hybrid multi-agent systems. *International Journal of Control, Automation and Systems*, 23(9):2503–2513, 2025.

[19] Siriluk Donganont, Uamporn Witthayarat, and Mana Donganont. Impulsive protocols for scaled consensus in edge-dynamic multi-agent systems. *European Journal of Pure and Applied Mathematics*, 18(1):5755, 2025.

[20] Mana Donganont. Distributed complex consensus in hybrid networks: A complex laplacian-based approach. *Asian Journal of Control*, n/a(n/a).

[21] Dennis S. Bernstein. *Matrix Mathematics: Theory, Facts, and Formulas*. Princeton University Press, Princeton, NJ, 2nd edition, 2009.

[22] Hassan K. Khalil. *Nonlinear Systems*. Prentice Hall, Upper Saddle River, NJ, 3rd edition, 2002.

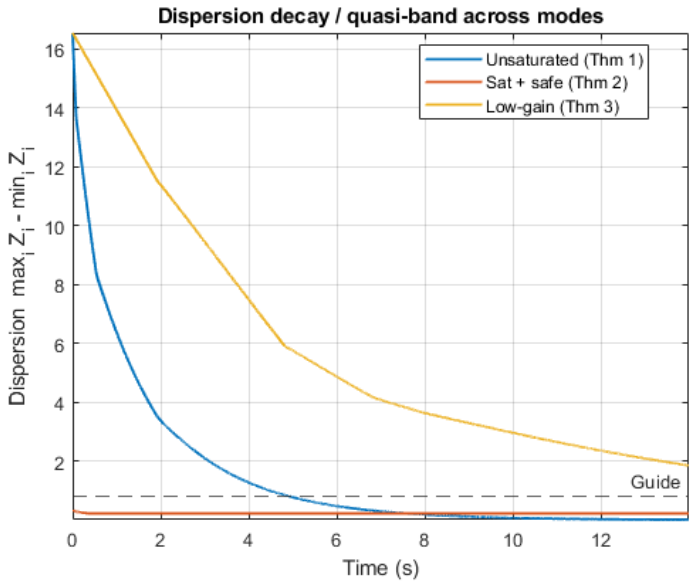

Figure 5: Dispersion evolution across regimes. The unsaturated case (blue) exhibits the fastest exponential decay; the safe-saturation case (orange) follows the same trajectory within the linear region; and the low-gain case (yellow) converges to a bounded quasi-band. The dashed reference line denotes the theoretical quasi-radius $\rho = c_q \alpha$, illustrating the accuracy of the analytical prediction.